DK-Iteration Robust Control of 2D Quadcopter

Tor Børve Rasmussen

***Abstract*—This paper presents a robust controller for controlling a simplified 2D quadcopter. Due to modelling errors uncertainties in the actuation efforts and moment of inertia is considered. A performance objective is defined and DK-iteration is used to achieve robust performance and stability. The controller is simulated and compared with a nominal controller. It is shown that the nominal controller is not able to achieve the same robust performance even after retuning.**

I. Introduction

THERE is an increasing interest for using quadcopters and other unmanned aerial vehicles (UAVs) in industry. Quadcopters are being, and has been proposed to be, used for several tasks like inspection of electric poles [1] and in congested areas [2]. Control is an essential part of these systems because if the system becomes unstable then it can have catastrophic consequences. The dynamics of a quadcopter is highly nonlinear due to aerodynamics and other external forces like gravity. Quadcopters are also susceptible to large disturbances like wind gust. The problem can also be ill-condition [3], i.e. that the force to pitch the quadcopter is much small then the force to change the elevation. Moreover, the parameters of the drone might change if the drone has a variable payload, like if it is used for delivery [4]. It is challenging to design a controller that is effective in such a wide range of scenarios.

There are several methods to control a quadcopter ranging from classical control methods [5] to advanced controllers which has been research for many years now. Model predictive control [6], gain scheduling [7], robust control [8] are some of the controllers used.

The quadcopter system analysed in this paper is a simplified linear 2D elevation and pitch model, which was derived in [9]. The two inputs, $\tilde{u}_f$ and $\tilde{u}_b$, are related to the lift forces produced by the front and rear motor respectively. The outputs are the elevation and pitch. The system is depicted as a block diagram in Fig. 2 and as a free body diagram in Fig. 1. This paper is organized as follows: In section II an uncertain model is described. In section III a robust controller for the system is presented. Finally in section IV simulation results are presented.

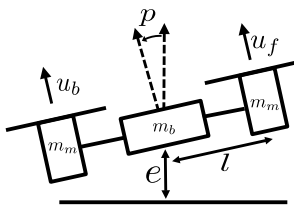

Fig. 1: Free body diagram of Quadcopter

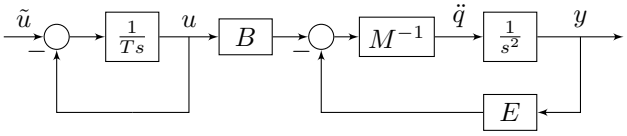

Fig. 2: Block diagram of linearized system.

II. Model Derivation

In [9] a linearized model was derived for the 2D quadcopter system. The system is summarized in Fig. 2, where $\tilde{u} = [\tilde{u}_f, \tilde{u}_b]^T$ is the applied input, u are the lift forces, $\ddot{q} = [\ddot{e}, \ddot{p}]^T$ and $y = [e, p]^T$. Furthermore, the the matrices $\mathbf{M}$, $\mathbf{E}$ and $\mathbf{B}$ are defined bellow. Where m_b is the mass of the body, m_m is the mass of one motor and l is the distance from the center to each motor as depicted in Fig. 1

$$\mathbf{E} = \begin{bmatrix} 0 & -g(m_b + 2m_m) \\ 0 & 0 \end{bmatrix}, \mathbf{B} = \begin{bmatrix} \sqrt{2}/2 & \sqrt{2}/2 \\ l & -l \end{bmatrix}$$
$$\mathbf{M} = \begin{bmatrix} m_b + 2m_m & 0 \\ 0 & 2l^2 m_m \end{bmatrix} \tag{1}$$

There are always discrepancies between the real system and a mathematical model of the system. This leads to uncertainties in the model. This system is no exception. The uncertainties are due to several reasons. One major reason is that the derived nonlinear model was linearized. Furthermore, the modelling was also heavily simplified in the first place. The quadcopter is not three point masses and the motors thrust can not be modelled exactly as a first order system as the real thrust depends on complicated aerodynamics and motor dynamics. In addition to this the values of T, m_m, m_b and l are all measured which introduces uncertainties as well. These uncertainties can be referred to as dynamic perturbations. The second category of model uncertainties comes from disturbance signals [10]. This can come from input output disturbances, sensor noise and actuator noise.

In this paper we will consider three dynamic perturbations. One for each of the motors and one for the moment of inertia around the pitch axis. These are chosen since they are believed to be the largest sources of uncertainty in the model.

As discussed the actuators are modelled as a simple first order systems, while in reality the generated lift depends on aerodynamics and internal motor dynamics. Furthermore, the uncertainty can represent the modelling errors due to the linearization. The full nonlinear model only is nonlinear due to the fact that the elevation acceleration is scaled by $cos(p)$[9]. Therefore, by adding uncertainties to the actuators we can to capture the modelling error due to the linearization. The actuators are therefore modelled with an output perturbation as follows

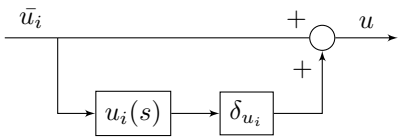

Fig. 3: Uncertainty in actuators

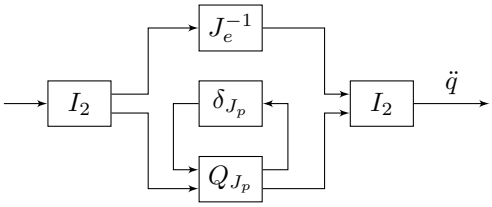

Fig. 4: Uncertainty in moment of inertia

$$u_i = \bar{u}_i(1 + p_{u_i}(s)\delta_{u_i}), i = 1, 2 \tag{2}$$

Where $\bar{u_i}$ is the nominal thrust force generated by the motor. $p_{u_i}(s)$ is the relative uncertainty. At low frequencies we have better knowledge about dynamics of the motors than at high frequencies due to transients and other unmodelled dynamics. Therefore, $|p_{u_i}(s)|$ should be larger at high frequencies. It was chosen that $|p_{u_i}(j0)| = 0.25$, $|p_{u_i}(j\infty)| = 0.9$ and $|p_{u_i}(j20)| = 0.575$. This gives the transfer function

$$p_{u_i}(s) = \frac{0.9s + 6.69}{s + 26.74}, i = 1, 2 \tag{3}$$

δ_{u_i} is the dynamic perturbation. It is complex a perturbation where $\delta_{u_i} \in \mathcal{C}$ and $\|\delta_{u_i}\|_{\mathcal{H}_\infty} \leq 1$. The actuator dynamics with the uncertainty dynamics added is depicted in Fig. 3

The second type of dynamic perturbation considered in this paper is the uncertainty in the moment of inertia around the pitch axis. From (1) we can see that the moment of inertia is $2l^2m_m$, however this is assuming that the that the body is a point mass in the center of the axis, and thus does the contribution to the moment of inertia is zero. However, in reality the body will add to to the moment of inertia. Furthermore, the motors are not point masses either. In practice it is possible to do experiments to determine the moments of inertia [11], however the configuration of the quadcopter might change at a later stage or the controller is used on a different quadcopter. Therefore, we would like to model this uncertainty. The reason for an uncertainty in the elevation acceleration is not considered is that this simply depends on the total mass of the quadcopter which can be easily measured very accurately.

Lets denote $\bar{J}_p = 2l^2m_b$ as the nominal moment of inertia around the pitch axis. From Fig. 2 we see that it is $\mathbf{M^{-1}}$ that affects the dynamics and not $\mathbf{M}$. Therefore, it is $\bar{J}_p^{-1}$ that affects the dynamics, however we want express the uncertainty as

$$J_p = \bar{J}_p(1 + p_{J_p}\delta_{J_p}) \tag{4}$$

where J_p is the actual moment of inertia, p_{J_p} is the relative uncertainty and was chosen as $p_{J_p} = 0.2$, finally δ_{J_p} is a real dynamic perturbation satisfying $\delta_{J_p} \in \mathcal{R}$ and $\|\delta_{J_p}\|_{\mathcal{H}_\infty}$. The expression for J_p^{-1} can be represented using an upper linear fractional transform (LFT)[10].

$$\begin{aligned} J_p^{-1} &= \mathcal{F}_U(Q_{J_p}, \delta_{J_p}) \\ J_p^{-1} &= Q_{J_p,22} + Q_{J_p,21}\delta_{J_p}(1 - Q_{J_p,11}\delta_{J_p})^{-1}Q_{J_p,12} \end{aligned} \tag{5}$$

$$\begin{aligned} Q_{J_p,11} &= -p_{J_p}, Q_{J_p,12} = \bar{J}_p^{-1}, \\ Q_{J_p,21} &= -p_{J_p}, Q_{J_p,22} = \bar{J}_p^{-1} \\ Q_{J_p} &= \begin{bmatrix} Q_{J_p,11} & Q_{J_p,12} \\ Q_{J_p,21} & Q_{J_p,22} \end{bmatrix} = \begin{bmatrix} -p_{J_p} & \bar{J}_p^{-1} \\ -p_{J_p} & \bar{J}_p^{-1} \end{bmatrix} \end{aligned} \tag{6}$$

In block diagram form the $\mathbf{M}^{-1}$ block can now be substituted with the system show in Fig. 4

The modelled quadcopter system has two measurements, $y = [e, p]^T$. In reality both these measurements will be corrupted by noise. The noise is modelled as additive bounded noise

$$y = \begin{bmatrix} e + W_e\delta_e \\ p + W_p\delta_p \end{bmatrix} \tag{7}$$

where $W_e = 0.1$, $W_p = 1°$, $\|\delta_e\|_{\mathcal{H}_\infty} \leq 1$ and $\|\delta_p\|_{\mathcal{H}_\infty} \leq 1$. The references for the elevation and pitch is also considered disturbances and is modelled as $e_r = W_{e_r}\delta_{e_r}$ and $p_r = W_{p_r}\delta_{p_r}$ where $W_{e_r} = 1$, $W_{p_r} = 45°$, $\|\delta_{e_r}\|_{\mathcal{H}_\infty} \leq 1$ and $\|\delta_{p_r}\|_{\mathcal{H}_\infty} \leq 1$.

III. Controller Design

The controller proposed in this paper is a μ-controller that tries to achieve the best possible robust performance. The controller is found in an iterative manner using DK-iteration [3].

There are two measurements available from the plant, elevation and pitch. Additionally the controller aims track a elevation- and pitch-reference. Instead of feeding the controller with the elevation- and pitch-error, it is provided with both the references and measurements separately. This gives the controller a larger degree of freedom compared to only providing the error-states. Thus the measurement y_K is defined as

$$y_K = [e_r, p_r, e, p]^T \tag{8}$$

Furthermore, it is necessary to define a performance objective. The most important objective is that $e_e = e_r - e$ and $e_p = p_r - p$ is small. Moreover, we want the error-states to be small at low frequencies. At higher frequencies we are not able to track the reference and thus should not have a significant weight on these frequencies. The weighting function used for the pitch error was chosen as

$$W_{pref,p}(s) = \frac{10^{-5}s + 0.1654}{s + 0.0058} \tag{9}$$

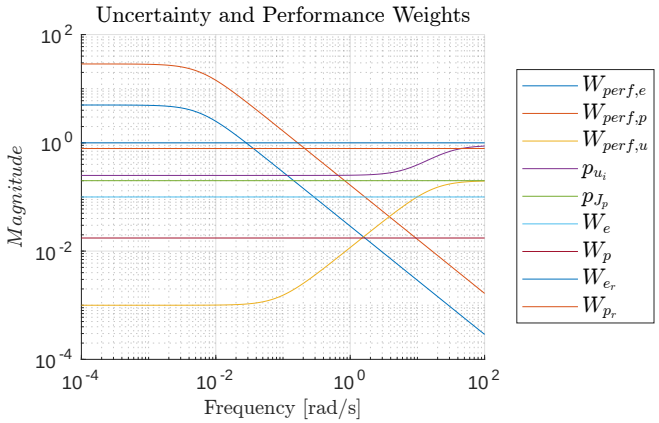

Fig. 5: Model uncertainties scales and performance weights

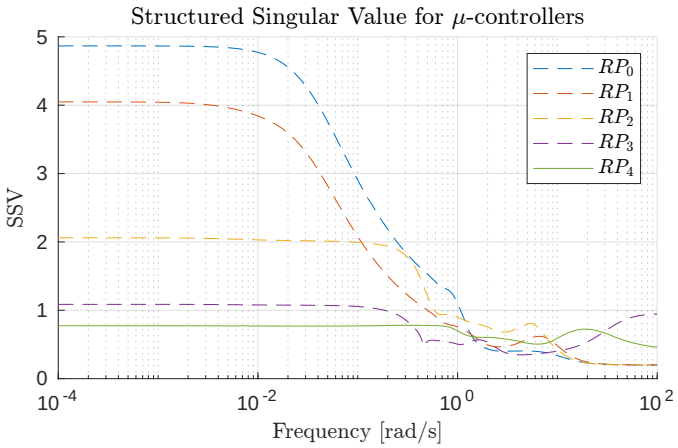

Fig. 6: Evolution of robust performance of μ controller

This weight satisfies that $W_{perf,p}(j0) \approx 28.65$ and starts rolling of at $\omega = 10^{-2}$ towards $W_{perf,p}(j\infty) = 10^{-5}$. For the elevation error a similar weight function was chosen

$$W_{perf,e}(s) = \frac{10^{-5}s + 0.0289}{s + 0.0058} \tag{10}$$

$W_{perf,e}(s)$ also rolls of at $\omega = 10^{-2}$ towards 10^{-5}, however at low frequencies we have that $W_{perf,e}(j0) = 5$. Thus, the pitch error is weighted more at low frequencies.

Other than the tracking of the references we also want the controller to limit the amount of actuation it uses, especially at higher frequencies. This will give the drone longer flight-time and also make the controller less aggressive. Therefore, $W_{perf,u}(s)$ was designed such that $W_{perf,u}(j0) = 1/1000$, $W_{perf,u}(j10) = 1/10$ and $W_{perf,u}(j\infty) = 1/5$. This yields the transfer function

$$W_{perf,u}(s) = \frac{0.2s + 0.0172}{s + 17.21} \tag{11}$$

The uncertainty weights and performance weights is depicted in Fig. 5

The μ-Synthesis toolbox [12] is used to implement the DK-Iteration algorithm. For the given problem the dynamic perturbation, Δ, takes the form $\Delta = diag\{[\delta_{u_1}, \delta_{u_2}, \delta_{J_p}]\}$. Furthermore, the performance perturbation, Δ_p, is a full block complex pertubration, i.e. $\Delta_p \in \mathcal{C}^{4\times4}$. Since the D-scales, D, has to commute with $\tilde{\Delta} = blkdiag\{[\Delta, \Delta_p]\}$, it has to take the form

$$D = diag\{[D_1, D_2, D_3, D_4, D_4, D_4, D_4]\} \tag{12}$$

A transfer function with order chosen in the range 0 to 4 was fitted to each element of D at each iteration such that

$$\hat{D}_i(j\omega) \approx D_i(\omega), \forall i = 1, 2, 3, 4 \tag{13}$$

IV. Simulation Results

In total four DK-iterations was achieved. For each iteration the robust performance got slightly better. The evolution of the structured singular values for the robust performance, RP, is depicted in Fig. 6. One can clearly see that μ is decreased drastically from the first iteration to the last. Importantly the peak of the robust performance for the μ-controller at the last iteration is 0.78. Thus the robust performance criteria is met and the closed loop system is robustly stable. Comparing the structured singular values with the LQR we see in Fig. 7 that the LQR does not meet the robust performance criteria. Furthermore, it is also not robustly stable.

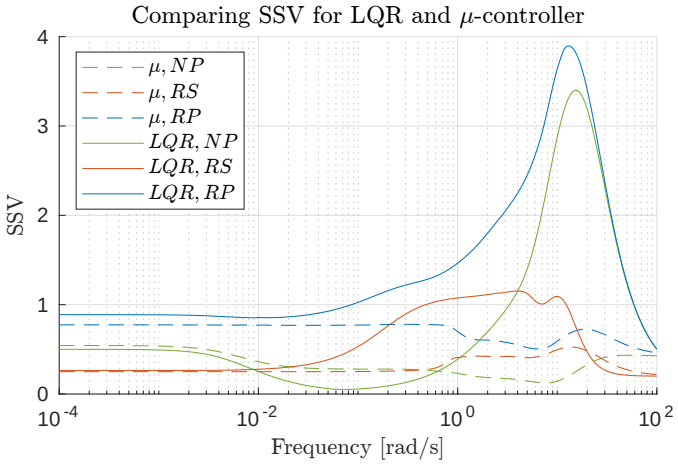

Fig. 7: Structured Singular Values for LQR and μ controller

Comparing the nominal elevation step responses depicted in Fig. 8 we see that the response using the μ-controller is quite similar to the LQR response. The μ-controller is less aggressive and thus starts climbing slower, however it still settles at the reference after a similar amount of time. However, looking at the actuation we see that the μ-controller uses much less actuation than the LQR, while still achieving similar performance.

The nominal pitch response is depicted in Fig. 9. The LQR has some overshoot, but converges in a similar time as the μ-controller. Looking at the actuation efforts we can see that they are very similar, almost identical. However, the pitch response is not that similar. This illustrates the point that the plant is ill-conditioned as discussed in section I.

By extracting the perturbation corresponding to the worst robust stability for both the closed loop LQR and μ-controller system, we find the worst case perturbation for both systems. In both cases it was found that the worst case perturbation is

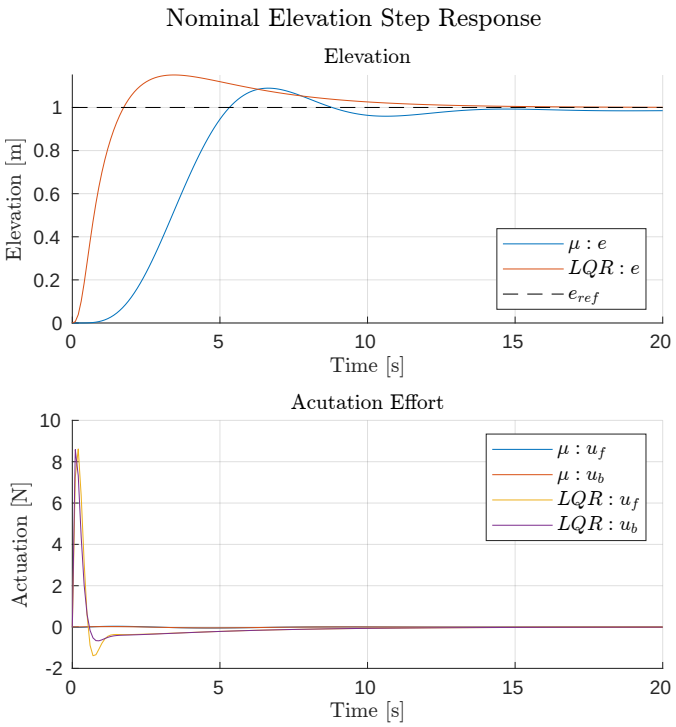

Fig. 8: Nominal elevation step response for LQR and μ-controller

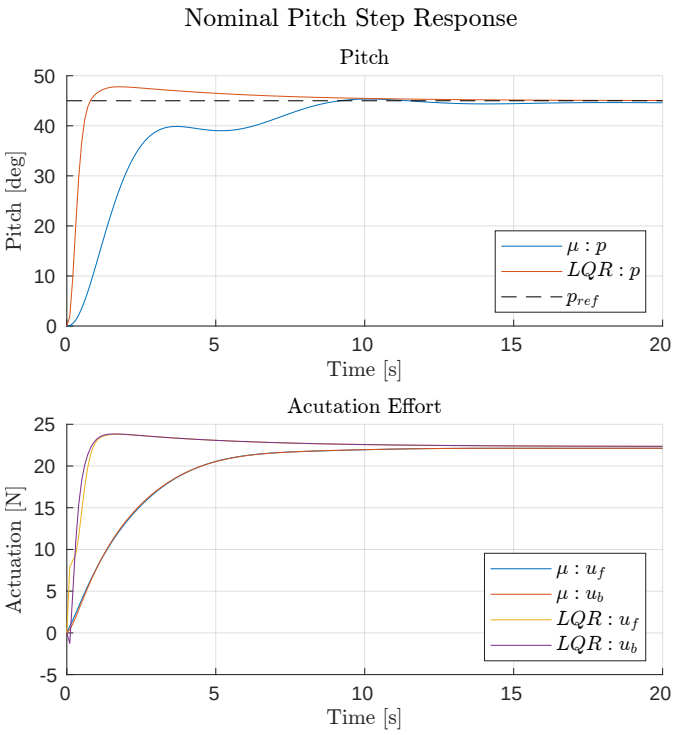

Fig. 9: Nominal pitch step response for LQR and μ-controller

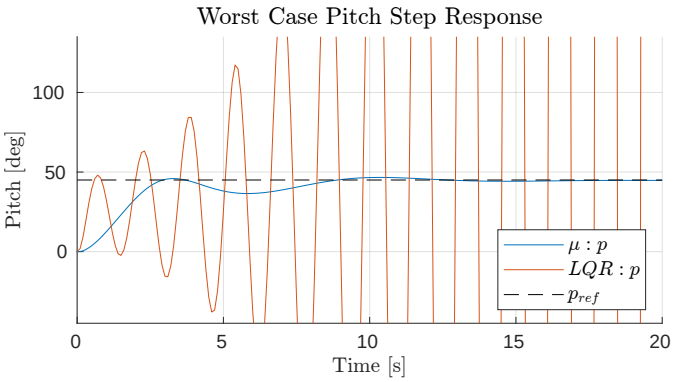

Fig. 10: Pitch step response of worst case perturbed system

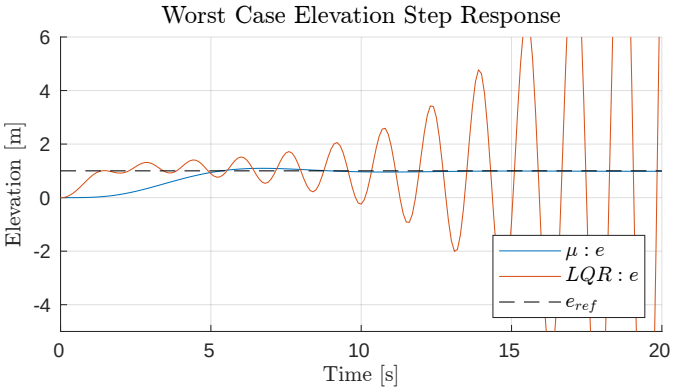

Fig. 11: Pitch step response of worst case perturbed system

when

$$\Delta_{WC} = \begin{bmatrix} 1 & 0 & 0 \\ 0 & -1 & 0 \\ 0 & 0 & 1 \end{bmatrix} \tag{14}$$

This corresponds to the front actuator, u_f, has the largest possible gain, the rear actuator, u_b, has the smallest possible gain, and lastly that the the moment of inertia around the pitch axis is at its maximum possible value. The fact that the perturbation on the actuators has the opposite sign indicates that it is mainly targeting the stability of the pitch axis since the actuator perturbations will cancel out for the elevation dynamics.

As predicted we see from Fig. 11 that the LQR becomes unstable in the presence of the worst case perturbation. We see that the pitch angle quickly diverges. On the other side the μ-controlled system is still stable. The performance is a bit degraded, however it still achieves a very impressive performance given the perturbations.

The story is similar for the elevation as depicted in Fig. 10. The μ-controller still achieves very good performance with no significant difference from the nominal response. By comparing the responses directly one can see that they are in fact very similar, within 10cm at all times. This is impressive, however not that surprising since as stated the actuators perturbations in the worst case perturbation (14) cancels for the elevation dynamics. Furthermore, the third perturbation only affects the pitch moment of inertia. Thus,

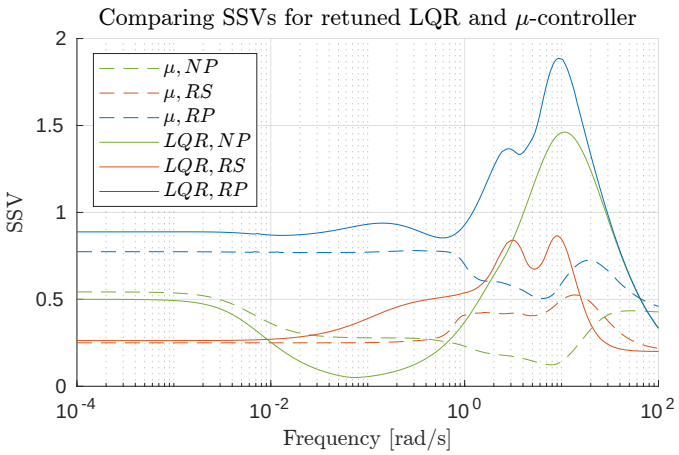

Fig. 12: Structured singular values of μ-controller and retuned LQR

the affect on the elevation dynamics is only indirect through the degraded pitch response.

A. Comparison with Retuned LQR

However, this comparison is quite unfair since the LQR was not designed to be particularly robust nor was it designed to fit the specific performance objective defined in this paper. Due to this the LQR proposed in [9] was retuned to for the defined performance objective and dynamic perturbations. The weights of the LQR was changed from $\mathbf{Q} = diag\{[10^2, 10^2, 10^3, 10^1, 10^3, 10^2, 1, 1]\}$, $\mathbf{R} = diag\{[1, 1]\}$ to $\mathbf{Q} = diag\{[10^2, 10^3, 10^3, 10^2, 10^2, 10^3, 10, 10]\}$, $\mathbf{R} = diag\{[30, 30]\}$. This was found to give the best robust performance.

As we can see from Fig. 12 the retuned LQR is better than the previous nominal controller. In fact the retuned controller is robustly stable, however it does not satisfy the robust performance criteria. From Fig. 13 we can see that the worst case elevation response of the retuned LQR still achieves good performance. For the pitch we can see in Fig. 14 that it struggles to converge to the reference, however it does so eventually. For the simulated worst case scenarios there is no noise on the measurements, however the μ-controller is designed to handle noise. The systems were therefore a simulated with noise. The noise was generated as a random choice between the maximum allowed and minimum allowed value of the bounds specified in (7). From Fig. 15 we can see that both controllers are now struggling to keep the elevation steady. From Fig. 16 we see that the pitch response is also much worse. The most significant difference between the two controllers is the actuation efforts. The LQR has a much higher control bandwidth, while the μ-controllers actuation efforts are more smooth. As specified in (11) we want to limit the actuation the controller uses at high frequencies. The fact that the LQR uses a higher control bandwidth is also deemed the reason why the robust and nominal performance depicted in Fig. 12 is bad at higher frequencies. This problem could perhaps be alleviated if the LQR was designed to control the derivative of the actuation instead of the actuation directly,

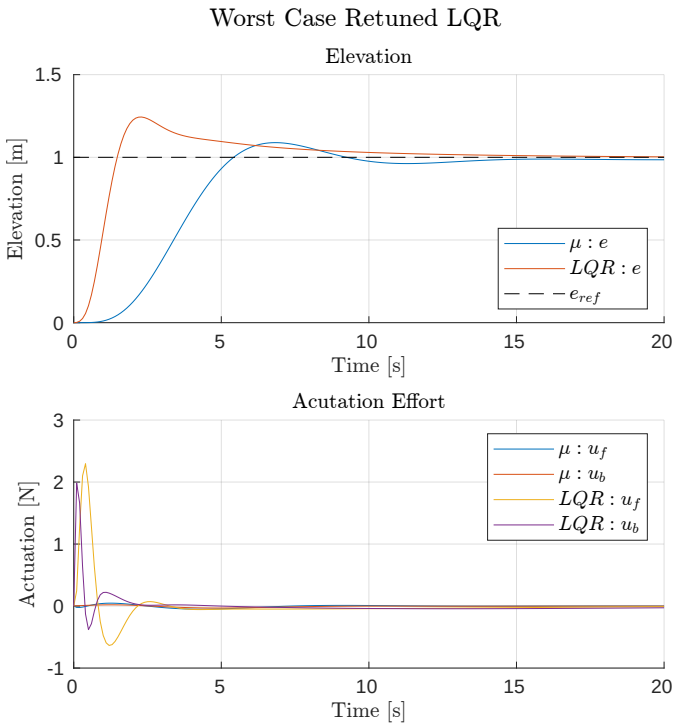

Fig. 13: Elevation step response of worst case perturbed system for retuned LQR and μ-controller without noise

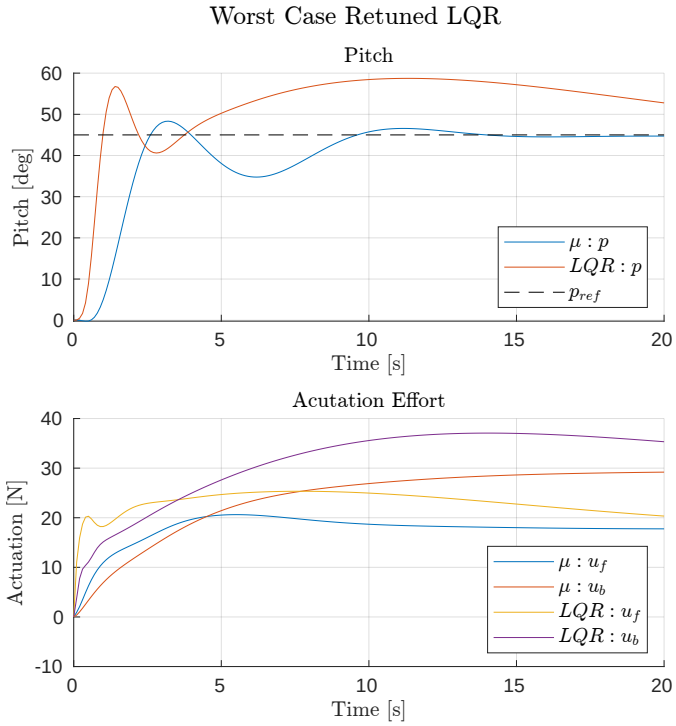

Fig. 14: Pitch step response of worst case perturbed system for retuned LQR and μ-controller without noise

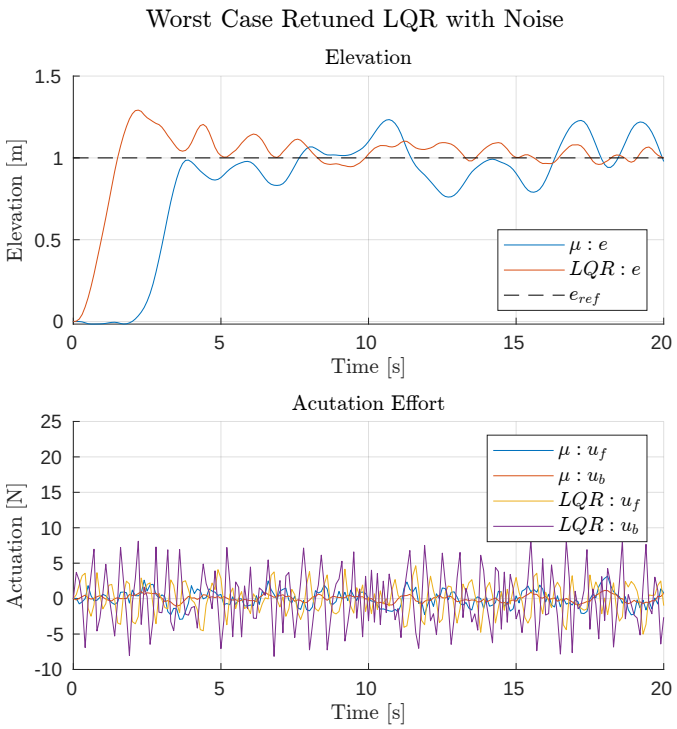

Fig. 15: Elevation step response of worst case perturbed system for retuned LQR and μ-controller with noisy measurements

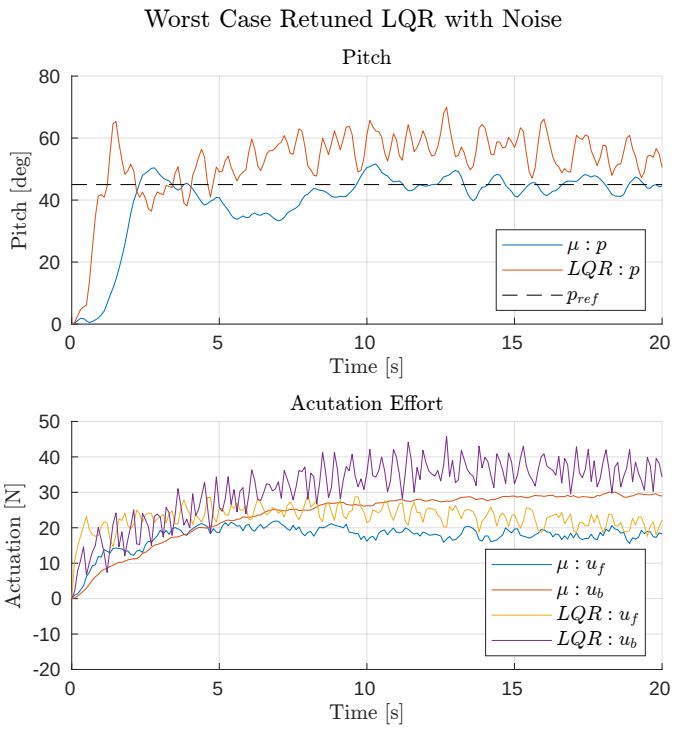

Fig. 16: Pitch step response of worst case perturbed system for retuned LQR and μ-controller with noisy measurements

however this was not evaluated. Lastly note that the controllers are simulated using the linearized system. It is not certain that the performance and stability results discussed in this section applies for the nonlinear system.

V. Conclusion

The robust, μ-synthesis approach has been used to design a robust controller for a 2D quadcopter system. The controller was designed to handle uncertainties in the actuators as well as the moment of inertia around the pitch axis. A total of four DK-iterations was achieved, where the robust performance was improved for each iteration. The final controller achieves the specified robust performance criteria. The robust controller was compared to a nominal LQR controller. It was shown that the LQR was not able to match the robust performance of the μ-controller, even after retuning. Moreover, the two closed loop systems was simulated and compared. The LQR was shown to have a similar nominal tracking performance as the μ-controller. Lastly, the closed loop system in the presence of the worst-case perturbation was then simulated with noise. It was shown that the performance of the LQR was severely degraded due to high frequencies in the actuation efforts. On the other hand the performance of the μ-controller was still good.

References

[1] I. Sa and P. Corke, "Vertical infrastructure inspection using a quadcopter and shared autonomy control," vol. 92, 01 2012.

[2] H. Goudarzi, D. Hine, and A. Richards, "Mission automation for drone inspection in congested environments," in *2019 Workshop on Research, Education and Development of Unmanned Aerial Systems (RED UAS)*, 2019, pp. 305–314.

[3] S. Skogestad and I. Postlethwaite, *Multivariable feedback control: analysis and design*. John Wiley & Sons, 2005.

[4] N. T. K. Chi, L. T. Phong, and N. T. Hanh, "The drone delivery services: An innovative application in an emerging economy," *The Asian Journal of Shipping and Logistics*, vol. 39, no. 2, pp. 39–45, 2023. [Online]. Available: https://www.sciencedirect.com/science/article/pii/S2092521223000020

[5] H. Bolandi, M. Rezaei, R. Mohsenipour, H. Nemati, and S. M. Smailzadeh, "Attitude control of a quadrotor with optimized pid controller," *Scientific Research*, vol. 4, no. 3, 2013. [Online]. Available: https://www.scirp.org/journal/paperinformation?paperid=35654

[6] A. Romero, S. Sun, P. Foehn, and D. Scaramuzza, "Model predictive contouring control for near-time-optimal quadrotor flight," *CoRR*, vol. abs/2108.13205, 2021. [Online]. Available: https://arxiv.org/abs/2108.13205

[7] J. Luengo, J. Bordeneuve-Guibé, F. Defay, and ISAE-Supaéro, "Model reference adaptive and gain scheduling control for variable payload uav quadcopters," 2019. [Online]. Available: https://api.semanticscholar.org/CorpusID:211093426

[8] V. N. Sankaranarayanan, S. Satpute, and G. Nikolakopoulos, "Adaptive robust control for quadrotors with unknown time-varying delays and uncertainties in dynamics," *Drones*, vol. 6, no. 9, 2022. [Online]. Available: https://www.mdpi.com/2504-446X/6/9/220

[9] T. B. Ramussen, "Optimal control and modelling of 2d quadcopter," 2024.

[10] T. Roy and R. K. Barai, "Control oriented lft modeling of a non linear mimo system," 2013. [Online]. Available: https://api.semanticscholar.org/CorpusID:212549373

[11] Setati, Tiro, Botha, Natasha, and Roux, Jeanne Marie, "Experimental approach to calculate the moments of inertia of a hexacopter unmanned aerial vehicle," *MATEC Web Conf.*, vol. 370, p. 05001, 2022. [Online]. Available: https://doi.org/10.1051/matecconf/202237005001

[12] G. J. Balas, J. C. Doyle, K. Glover, A. Packard, and R. Smith, "μ-analysis and synthesis toolbox," *MUSYN Inc. and The MathWorks, Natick MA*, vol. 72, 1993.